Carbon Monoxide and Nitric Oxide Mediate Cytoskeletal Reorganization in Microvascular Cells via Vasodilator-Stimulated Phosphoprotein Phosphorylation

Evidence for Blunted Responsiveness in Diabetes

Sergio Li Calzi,[1] Daniel L. Purich,[2] Kyung Hee Chang,[1] Aqeela Afzal,[1] Takahiko Nakagawa,[3] Julia V. Busik,[4] Anupam Agarwal,[3] Mark S. Segal,[5] and Maria B. Grant[1]

OBJECTIVE—We examined the effect of the vasoactive agents carbon monoxide (CO) and nitric oxide (NO) on the phosphorylation and intracellular redistribution of vasodilator-stimulated phosphoprotein (VASP), a critical actin motor protein required for cell migration that also controls vasodilation and platelet aggregation.

RESEARCH DESIGN AND METHODS—We examined the effect of donor-released CO and NO in endothelial progenitor cells (EPCs) and platelets from nondiabetic and diabetic subjects and in human microvascular endothelial cells (HMECs) cultured under low (5.5 mmol/l) or high (25 mmol/l) glucose conditions. VASP phosphorylation was evaluated using phosphorylation site-specific antibodies.

RESULTS—In control platelets, CO selectively promotes phosphorylation at VASP Ser-157, whereas NO promotes phosphorylation primarily at Ser-157 and also at Ser-239, with maximal responses at 1 min with both agents on Ser-157 and at 15 min on Ser-239 with NO treatment. In diabetic platelets, neither agent resulted in VASP phosphorylation. In nondiabetic EPCs, NO and CO increased phosphorylation at Ser-239 and Ser-157, respectively, but this response was markedly reduced in diabetic EPCs. In endothelial cells cultured under low glucose conditions, both CO and NO induced phosphorylation at Ser-157 and Ser-239; however, this response was completely lost when cells were cultured under high glucose conditions. In control EPCs and in HMECs exposed to low glucose, VASP was redistributed to filopodia-like structures following CO or NO exposure; however, redistribution was dramatically attenuated under high glucose conditions.

CONCLUSIONS—Vasoactive gases CO and NO promote cytoskeletal changes through site- and cell type–specific VASP phosphorylation, and in diabetes, blunted responses to these agents may lead to reduced vascular repair and tissue perfusion. ***Diabetes*** **57:2488–2494, 2008**

From the [1]Department of Pharmacology and Therapeutics, University of Florida, Gainesville, Florida; the [2]Department of Biochemistry & Molecular Biology, University of Florida, Gainesville, Florida; the [3]Department of Medicine, Nephrology Research and Training Center, University of Alabama at Birmingham, Birmingham, Alabama; the [4]Department of Physiology, Michigan State University, East Lansing, Michigan; and the [5]Department of Nephrology, University of Florida, Gainesville, Florida.

Corresponding author: Maria B. Grant, grantma@ufl.edu.

Received 18 March 2008 and accepted 7 June 2008.

Published ahead of print at http://diabetes.diabetesjournals.org on 16 June 2008. DOI: 10.2337/db08-0381.

The gaseous signal molecules nitric oxide (NO) and carbon monoxide (CO) exert multiple modulatory actions in regulating vascular function. While NO effects have been recognized for over a decade, similar vasoregulatory action of CO was established only recently. CO is generated by heme oxygenase (HO)-1 under a wide variety of conditions (e.g., cell exposure to such stressors as hypoxia, growth factors, and cytokine stimulation) that activate the enzyme (1,2). Unlike its highly reactive cognate NO, which participates in multiple redox reactions, CO is a relatively stable gas that exhibits extraordinary affinity for heme centers (3–5). Like NO, the signaling effects of CO rely in part on its ability to form a complex with the heme moiety of soluble guanylate cyclase (sGC), stimulating the synthesis of the diffusible second messenger guanosine 3′5′-cyclic monophosphate (cGMP) (6). The sGC/cGMP pathway plays a critical role in mediating the effects of CO on vascular relaxation and inhibition of platelet aggregation and coagulation (7,8).

A recently recognized property of NO is its cell type–specific facilitation or inhibition of cell migration (9), a complex process involving molecular-mechanical events that depend on extracellular signaling, actin-based motility, and cell adhesion. Endothelial progenitor cells (EPCs) differentiate into endothelial cells whose function in vascular repair depends on chemokine- and growth factor–directed cell migration. The role of EPCs in endothelial repair is supported by their ability to inhibit development of atherosclerosis (10,11) and intimal hyperplasia (12), while still promoting beneficial angiogenesis. We previously demonstrated the central role of the actin cytoskeleton in EPC migration (13), and our findings suggest that NO has a critical function within EPCs, where it regulates the distribution of vasodilator-stimulated phosphoprotein (VASP). The latter plays a pivotal role in promoting actin filament elongation at the leading edge by forming an active molecular motor complex that propels motility (14). VASP contains three distinct phosphorylation sites (Ser-157, Ser-239, and Thr-278), the first of which is preferentially phosphorylated by cAMP-dependent protein kinase (PKA) and the second by cGMP-dependent protein kinase (PKG). Although the exact roles of phosphorylated residues in VASP have not completely been elucidated, one idea is that a high 3′,5′-cyclic AMP (cAMP)-to-cGMP ratio promotes VASP-activated actin filament elongation, whereas a low cAMP-to-cGMP ratio favors filament capping and loss of motility (15). The following factors are

known to influence VASP phosphorylation: intracellular localization in focal adhesions, filopodia, and lamellipodial; accessibility of phosphorylation sites in VASP that is complexed with other proteins; availability of specific protein kinases and/or phosphoprotein phosphatases; and the respective activators and inhibitors of these kinases and phosphatases (16). We previously reported that the reduced bioavailability of NO in diabetic individuals prevents VASP redistribution, resulting in the inability of EPCs to form proper cytoskeletal extensions (13). We also showed that the EPC chemoattractant stromal cell–derived factor-1 (SDF-1) transcriptionally activates HO-1 via the atypical protein kinase C (PKC)-ζ isoform generating CO, which in turn can phosphorylate VASP in endothelial cells (17).

Because PKG and PKA catalyze VASP phosphorylation, and because the latter is thought to control VASP's subcellular distribution and function (13), we directly compared the effects of NO and CO on VASP phosphorylation and redistribution in cells typically known to be dysfunctional in diabetes, namely platelets, EPCs, and microvascular endothelial cells. We demonstrate that both CO and NO regulate VASP phosphorylation and that pretreatment with either agent stimulates migration toward SDF-1. We also show that normal platelets display a modest response to exogenous CO stimulation but a greater response to NO treatment. In contrast, diabetic platelets are not responsive to either CO or NO treatment (data not shown). Culturing microvascular endothelial cells at high glucose concentrations also results in reduced VASP phosphorylation. These novel findings suggest that CO regulates VASP phosphorylation and vascular cell migration under conditions of reduced NO bioavailability, as observed in diabetes.

RESEARCH DESIGN AND METHODS

Cell culture. Human lung microvascular endothelial cells (HMECs) (LONZA, Walkersville, MD) were cultured to 80% confluency in EGM-2 MV medium (LONZA) in 5.5 or 25 mmol/l glucose for 1 week. Cells were then incubated overnight in EBM-2 supplemented with 2% fetal bovine serum. Fresh medium (EBM-2 + 2% fetal bovine serum) was added on the following day, and CO- or NO-containing medium was added to the designated samples for 1 or 15 min at 37°C, as described below.

Isolation of platelets. Peripheral blood from healthy and diabetic volunteers giving informed consent under a protocol approved by the institutional review board was collected in cell preparation tubes (CPTs) with heparin (BD Biosciences, San Jose, CA), and platelets were isolated using Opti-Prep (Axis-Shield PoC, Oslo, Norway), as recommended by the manufacturer.

EPC culture. Peripheral blood from healthy and diabetic volunteers was then collected into CPTs (BD Biosciences), and the EPCs were freed of the mononuclear cells using an Endocult medium kit (Stem Cell Technologies, Vancouver, CA) according to the manufacturer's protocol, as previously described (13).

Immunohistochemistry. EPCs were cultured onto fibronectin-coated dishes with Endocult stem cell liquid media until colonies formed. These cells were then treated for 15 min or 4 h with 100 μmol/l diethylenetriamine (DETA)-NO (Sigma-Aldrich, St. Louis, MO) in water or 10 μmol/l CO-donor $Ru(II)(CO)_3Cl_2$ (Sigma-Aldrich) in DMSO. Control samples were treated with vehicle. At the end of the treatment, medium was removed and cells were fixed overnight at 4°C in 4% paraformaldehyde in PBS, supplemented with calcium and magnesium ions, and adjusted to pH 7.4.

Cells were then washed in PBS and permeabilized with 0.1% Triton X-100 for 30 min at room temperature. After washing the samples an additional three times in PBS, cells were treated with 10% normal goat serum–1% BSA in PBS for 1 h at room temperature to block nonspecific antigens. Cells were then incubated with 5 μg/ml mouse anti-VASP antibody (BD Biosciences) in 5% normal goat serum overnight at 4°C and then with fluorescein isothiocyanate (FITC)-labeled goat anti-mouse IgG_1 (1:250 dilution) (Southern Biotech, Birmingham, AL) in 5% normal goat serum for 1 h at room temperature. Samples were then washed, dried, and mounted with 4′,6-diamino-2-phenylindole (DAPI) (Vectashield; Vector Laboratories, Burlingame, CA) to label nuclear DNA. Samples were examined by fluorescence microscopy (Nikon Eclipse TE200) using a Nikon Plan-fluor ×40 (NA = 1.30) oil objective and a fluorescein filter set (520 ± 2 nm). Micrographs were captured using a SPOT digital camera 0.60X HRD06-NIK (Diagnostic Instruments, Sterling Heights, MI) and processed using SPOT Advanced software Version 2.2.1 for Windows.

Fluorescence-activated cell sorting. Peripheral blood was collected into CPTs (BD Biosciences) and centrifuged to obtain the mononuclear cell fraction, from which $CD34^+$ cells were isolated using a $CD34^+$ isolation kit (Stem Cell Technologies, Vancouver CA). Briefly, 2×10^{-7} cells were incubated with a $CD34^+$ selection cocktail for 15 min, and 50 μl magnetic nanoparticles was then added and incubated for another 10 min. The suspension volume was increased to 2.5 ml, and the particle-bound $CD34^+$ cells were concentrated on the tube's inner surface with the aid of a magnet. The supernatant was decanted, and the remaining $CD34^+$ cells were resuspended in RPMI culture media (Cellgro, Herndon, VA).

The cells were then treated with 100 μmol/l on DETA-NO (Sigma-Aldrich) for either 15 min or 4 h in a CO_2 incubator. Following treatment, the $CD34^+$ cells were permeabilized using a cytofix/Cytoperm kit (BD Biosciences) and blocked with 10% normal human serum (Jackson Immuno Research labs, West Grove, PA), and 10 μg antiphospho-VASP (Upstate Signaling, Lake Placid, NY) was added to the cells, followed by 30-min incubation on ice. The cells were then washed with PBS and incubated with 23 μg FITC-conjugated goat anti-mouse (Jackson Immuno Research labs, West Grove, PA), and again incubated on ice for 30 min. The resulting cells were washed in PBS and analyzed by fluorescence-activated cell sorting (FACS). Anti-GFP (Molecular probes, Carlsbad, CA) was used as an isotype control.

Preparation of DETA-NO and $Ru(II)(CO)_3Cl_2$ donors. The half-lives for NO and CO release from DETA-NO and $Ru(II)(CO)_3Cl_2$ are greatly different, resulting in the almost immediate release of CO but very slow release of NO. Therefore, to assure that cells were exposed to comparable concentrations of NO and CO, we first calculated the amount of CO released at 1 and 15 min using the integrated rate law: $[\text{CO donor}]_t/[\text{CO donor}]_{\text{initial}} = \exp(-k_{CO}t)$, where $[\text{CO donor}]_t$ and $[\text{CO donor}]_{\text{initial}}$ are the CO donor concentrations at time t and, initially, k_{CO} is the first-order rate constant for CO release, and t is the incubation period. We then used the corresponding rate law, i.e., $[\text{NO donor}]_t/[\text{NO donor}]_{\text{initial}} = \exp(-k_{NO}t)$ to determine the time needed to obtain an extent of NO release comparable with that observed with CO donor in 1 and 15 min. The CO and NO donor rate constants k_{CO} and k_{NO} of 0.07 min^{-1} and 0.0006 min^{-1}, respectively, were determined based on the published half-lives of 10 min for $Ru(II)(CO)_3Cl_2$ (18) and 18 h for DETA-NO (19). In our experiments, we therefore separately preincubated the NO donor in culture medium in a sealed tube for the calculated NO times, and then transferred an appropriate aliquot to the cell. Because the partial pressure exerted by the released NO and CO is far below the solubilities in aqueous solution, and because the 1- and 15-min exposure times were short, there was no need to maintain treated cells in a sealed culture dish.

Immunoblot. Following treatment with either the CO or NO donor, the $CD34^+$ cells or platelets were washed with PBS and lysed with lysis buffer (Cell Signaling, Danvers, MA) containing protease (catalog no. P8340l Sigma-Aldrich) and phosphatase inhibitors (catalog no. P2850; Sigma-Aldrich). Protein was quantified in each sample using a commercially available BCA kit (Pierce, Rockford, IL), and 50 μg was applied to each well above the polyacrylamide gel (7.5%) (Criterion; Biorad Laboratories, Richmond, CA) at 120 V for 20 min, followed by 140 V for 65 min. Samples were run in duplicate for later detection of the two phosphorylated VASP (pVASP) isoforms. The separated proteins were transferred to a nitrocellulose membrane (Biorad Laboratories) in a semidry transblot apparatus (Biorad Laboratories). The membranes were blocked in Tris-buffered saline (TBS) containing 5% milk and 0.05% Tween-20 (Sigma-Aldrich) for 1 h at room temperature. For the detection of pVASP isoforms, the membranes were incubated at 4°C overnight with either a mouse monoclonal anti-pVASP Ser-239 antibody (Upstate Cell Signaling Solutions, Lake Placid, NY) or a rabbit polyclonal anti-pVASP Ser-157 antibody (Santa Cruz Biotechnology, Santa Cruz, CA), both at a 1:200 dilution. Blots were then washed with 5% milk for 5 min and incubated with a 1:2,000 dilution of either a horseradish peroxidase (HRP)-conjugated anti-mouse antibody (Sigma-Aldrich) or an anti-rabbit (Santa Cruz Biotechnology) for 1 h at room temperature. After incubation with the secondary antibody, the membranes were washed twice with TBS containing 0.05% Tween-20 for 5 min, followed by two additional 10-min washes with TBS. Protein bands were visualized with enhanced chemiluminescence using a commercial Western blot detection kit (Amersham Biosciences, Amersham, U.K.) and pVASP levels were quantified using Scionimage software (Scion, Frederick, MD). Standard molecular weight markers (Biorad Laboratories) served to verify the molecular mass of pVASP (50 kDa).

After pVASP detection, the membranes were reprobed for VASP using a 1:200 dilution of a goat anti-VASP antibody (Santa Cruz Biotechnology) and

for β-actin using a mouse anti–β-actin primary antibody at a dilution of 1:7,000 (Sigma-Aldrich), followed by HRP-conjugated anti-goat (Santa Cruz Biotechnology) and anti-mouse IgG antibody (Sigma-Aldrich), both at 1:2,000 dilution, and were visualized by enhanced chemiluminescence. Standard molecular weight markers served to verify the 42-kDa molecular mass of β-actin.

In-cell Western analysis. $CD34^+$ cells were cultured in defined serum-free medium (StemSpan SFEM; StemCell Technologies, Vancouver, Canada) to obtain an optimal number of cells. For $CD34^+$ cell proliferation and expansion, without differentiation, we used 1 ml StemSpan SFEM supplemented with a cytokine cocktail (100 ng/ml flt3 ligand, 100 ng/ml stem cell factor, 20 ng/ml interleukin-3, and 20 ng/ml interleukin-6; StemCell Technologies) and 50 ng/ml thrombopoietin (R&D Systems, Minneapolis, MN). After determining cell number with a hemocytometer (Hausser Scientific, Horsham, PA), 10,000 cells were transferred to each well in a 96-well plate (BD Falcon, San Jose, CA). After incubation with/without CO or NO donor, cells were fixed with 4% paraformaldehyde for 20 min at room temperature and then harvested by centrifugation. After removing the fixation solution, cells were permeabilized with 0.1% Triton X-100 in PBS and blocked with LI-COR Odyssey blocking buffer (LI-COR Biosciences, Lincoln, NE) for 1.5 h at room temperature with moderate shaking. Blocking buffer was removed by aspiration, and the cells were incubated with 50-μl volume of diluted primary antibody at 4°C overnight in a cold room. Cells were then washed four times for 5 min in PBS containing 0.1% Tween-20 (Fisher Scientific, Pittsburgh, PA) and incubated with diluted secondary antibody. After 1-h incubation, cells were washed four times (5 min each) with PBS containing 0.1% Tween-20, followed by final washing in PBS to remove excessive detergent. The 96-well plate was then scanned in the appropriate channels using an Odyssey infrared imaging system (LI-COR Biosciences). Relative quantification was normalized and readjusted in cell number from well to well using DNA staining.

Statistical analysis. All reported data are expressed as the mean ± SEM and were obtained from at least three independent experiments. Student's *t* test and ANOVA with Student-Newman-Keuls posttest were used to compare the data.

RESULTS

The choice of the technique used (e.g., standard Western blotting, In-Cell Western analysis, and FACS) for these studies was largely governed by the number of cells available for analysis. Because $CD34^+$ cells represented <1% of circulating mononuclear cells, In-Cell Western (low sensitivity) and FACS (higher sensitivity) analyses were the methods of choice; however, for more abundant cells such as endothelial cells, standard Western blotting was sufficient. All the phosphorylation studies on EPCs were performed after 15 min of treatment. We then tested whether a shorter treatment (1 min) could still elicit a significant migratory response.

We therefore pretreated human $CD34^+$ EPCs for 1 and 15 min with medium containing NO or freshly generated CO, followed by SDF-1 stimulation (13), and then assessed cell migration using Boyden chambers. As demonstrated in Fig. 1, both CO and NO treatment resulted in increased EPC migration to SDF-1, although a more robust response was observed with NO at 1 min.

Because VASP is a key component of the actoclampin molecular motors responsible for actin-based cell motility (14,20), and because VASP was originally identified as a major substrate for cGMP-stimulated protein kinase in platelets and endothelial cells (21), we investigated whether NO and CO elicited similar effects on VASP phosphorylation and its mobilization to the leading edge of motile cells. VASP function appears to be chiefly regulated by phosphorylation at Ser-157 and Ser-239, and the availability of phosphorylation site-specific antibodies provides an unambiguous way to define both the sites and extents of signal molecule–activated VASP phosphorylation. We therefore incubated $CD34^+$ cells for 15 min in the presence of NO or CO already liberated from their respective donors. As shown in Fig. 2, NO treatment routinely increased the extent of VASP phosphorylation at Ser-239,

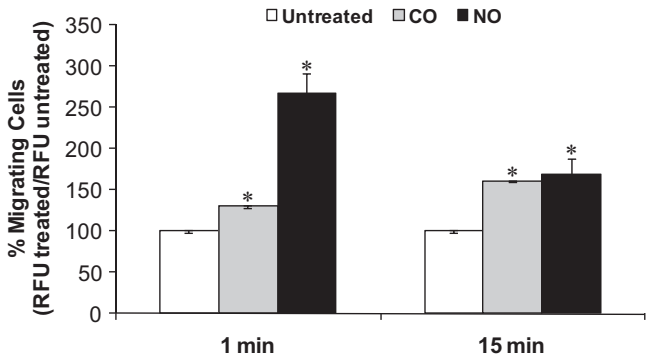

FIG. 1. CO or NO treatment of EPCs stimulates migration. Because the rate constants for CO release from $Ru(II)(CO)_3Cl_2$ dimer and for NO release from DETA-NO are so disparate (RESEARCH DESIGN AND METHODS), experiments with the NO donor required prior incubation for times sufficient to release equivalent concentrations of NO and CO. Accordingly, EPCs (obtained from healthy human subjects) were treated with 10 μmol/l $Ru(II)(CO)_3Cl_2$ dimer (CO donor) for 1 and 15 min, thereby generating 0.6 and 6.5 μmol/l CO, respectively. For the NO experiments, 100 μmol/l DETA-NO was first incubated in a sealed tube for 2 and 28 h (based on the calculated time required to generate 0.6 and 6.5 μmol/l NO, respectively), and then combined with EPC for 1 and 15 min, respectively. Cell migration in response to SDF-1 was subsequently assessed in a Boyden chamber. Representative results from at least three independent experiments are shown. Values represent means ± SD. *$P < 0.05$. RFU, relative fluorescence units.

whereas CO treatment consistently increased the extent of Ser-157 phosphorylation in these cells.

To confirm that the differential effects of CO and NO are not limited to $CD34^+$ cells, we also examined platelets, which are a rich source of VASP and are the cells wherein VASP phosphorylation is best characterized (22). In platelets exposed to either NO or CO for 1- and 15-min periods, we found that CO treatment caused a modest yet significant VASP phosphorylation at Ser-157, whereas NO treatment significantly increased VASP phosphorylation at Ser-157 with maximum response at 1 min and at Ser-239 with maximum effect at 15 min (Fig. 3). These findings suggest that CO and NO elicit markedly different VASP phosphorylation responses in platelets and $CD34^+$ cells.

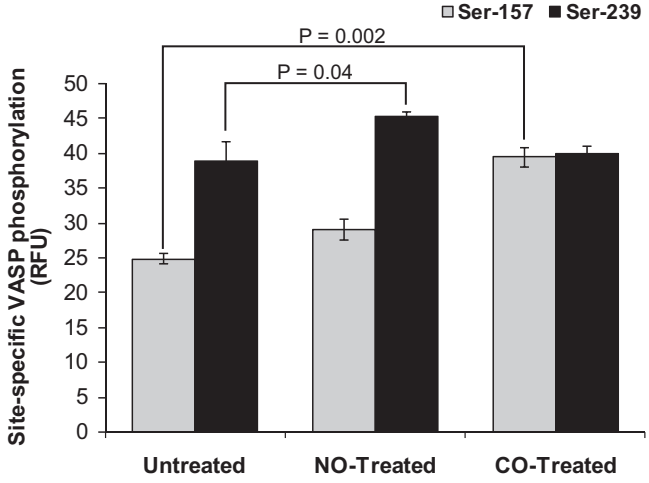

FIG. 2. Time course of NO- or CO-stimulated VASP phosphorylation at Ser-157 and Ser-239. $CD34^+$ cells were incubated for 15 min in the presence of either 6.5 μmol/l CO or NO (see legend to Fig. 1 for details), and protein extracts were analyzed by In-Cell Western (see RESEARCH DESIGN AND METHODS). Note that exposure of these cells to NO resulted in increased VASP phosphorylation at Ser-239, whereas CO increased phosphorylation at Ser-157. Representative results from four independent experiments are shown. Values represent means ± SD. Reported *P* values indicate significance between the treated and the corresponding untreated sample. RFU, relative fluorescence units.

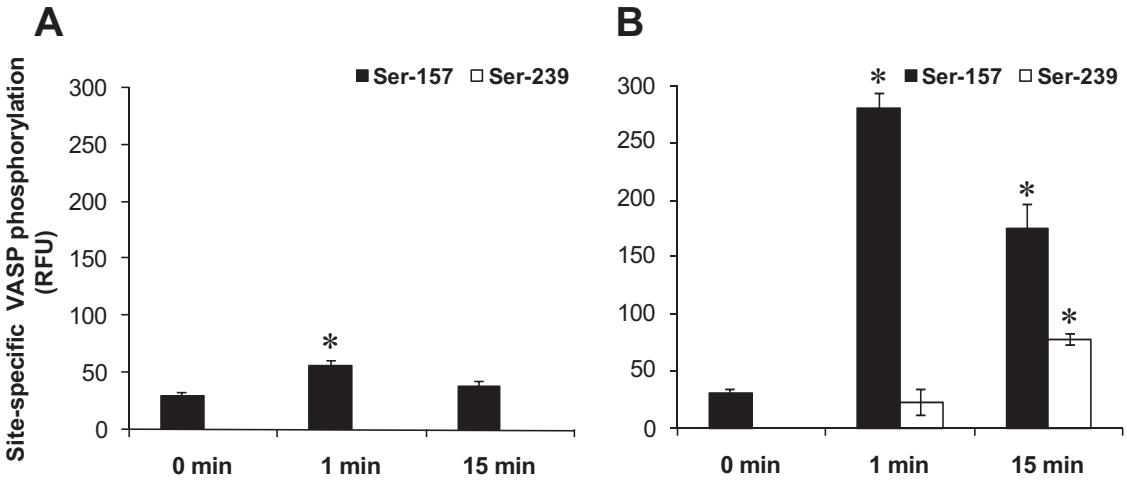

FIG. 3. Signal-mediated platelet VASP phosphorylation indicates low responsiveness to CO (*A*) but robust response to NO (*B*). Platelets (isolated from human peripheral blood as described above) were treated with either CO or NO as described in the legend to Fig. 1. Platelets were then extracted with lysis buffer, and equal quantities of total protein were loaded and separated by SDS-polyacrylamide gel electrophoresis, followed by transfer to nitrocellulose for immunoblotting with VASP phosphorylation site-specific antibodies. Corrections for variations in gel loading were made by normalizing band intensities to those for β-actin. Representative results from at least three independent experiments are shown. Values represent means ± SD. *$P < 0.05$. RFU, relative fluorescence units.

Because VASP resides on the cytoplasmic face of the leading edge in motile cells (23), and because VASP phosphorylation is believed to control its interactions with VASP-docking proteins like vinculin, zyxin, and migfilin, we next examined the effects of donor-generated NO and CO on the redistribution of VASP in microvascular endothelial cells growing while firmly adhered to fibronectin-coated culture dishes. Under basal conditions (i.e., no NO or CO), VASP was mainly localized along the sides of actin filaments found throughout the peripheral cytoplasm (Fig. 4*A* and *B*). However, following a 15-min exposure to CO, VASP redistributed to the leading edge of advancing microvascular endothelial cells (Fig. 4*C* and *D*). VASP redistribution was also observed when these cells were incubated with NO (Fig. 4*E* and *F*).

In as much as diabetes-associated vascular dysfunction is frequently attributed, at least in part, to reduced levels of bioavailable NO, we sought to determine whether diabetes impacted the NO and CO effects on VASP phosphorylation within cell types typically affected by diabetes. We treated platelet samples from diabetic individuals with NO or CO under the same conditions used in Fig. 1 and observed no change in VASP phosphorylation, at either Ser-157 or Ser-239 (data not shown). In Fig. 5, VASP phosphorylation is shown for two diabetic patients and one nondiabetic control subject. Patient 1 had type 2 diabetes of 5 years duration and excellent glycemic control (A1C 6.4%), while patient 2 had type 1 diabetes of 48 years duration and poor glycemic control (A1C 11.3%). A different pattern was observed in the diabetic $CD34^+$ cells, where NO treatment stimulated phosphorylation at VASP's Ser-239 to a significantly less extent, when compared with the nondiabetic control cells. However, we observed considerable patient-to-patient variation in the degree of the response but all with the same pattern.

Notably, compared with control cells grown in low-glucose medium, exposure of microvascular cells to conditions mimicking aspects of diabetes (e.g., culturing these cells for 1 week in high-glucose medium) resulted in a failure of NO and CO to elicit changes in either VASP redistribution to the leading edge of the cells, as shown by immunofluorescence (compare Figs. 4 and 6), or phosphorylation at Ser-157 or Ser-239, as detected by standard Western blot analysis (Fig. 7).

DISCUSSION

Understanding the regulation of endothelial cell migration in response to chemokines has proven to be a daunting task that requires the investigation of a manifold of factors known to affect chemotaxis (e.g., chemokine sensing by receptor-mediated signaling, cellular locomotion by actin-based molecular motors, and even the cell's energy status). Previous studies from our laboratory on $CD34^+$ EPCs showed that diabetic EPCs have reduced intracellular NO concentration as well as a concomitantly reduced migratory capability. We found that, when pretreated with an NO donor, cell migration can be restored (13), and we further demonstrated that this exogenous NO exposure resulted in enhanced diabetic cell migration, with attendant changes in phosphorylation of the actin cytoskeletal protein VASP (13).

Given the robust nature of the vasodilator gases CO and NO in modulating vascular function, we focused on the following questions: Can CO suffice in place of NO in promoting vascular cell migration? If so, do NO and CO exert their signaling effects on the same downstream phosphorylation target(s)? In this study, we demonstrate that CO can regulate VASP phosphorylation and in turn alter cell migration. We also directly compare the CO effects to those of NO in EPCs, platelets, and microvascular endothelial cells. Our studies demonstrate that both vasoactive gases promote cytoskeletal changes through site- and cell type–specific VASP phosphorylation; however, these responses to NO and CO are blunted in diabetes and may be responsible for reduced vascular repair and tissue perfusion (24,25).

The actoclampins are the force-generating motors responsible for actin-based cell crawling and vesicle motility (14). Each of these membrane surface–bound molecular motors consists of an actin filament plus-end tracking protein called a clampin (e.g., VASP, N-WASP [neural Wiskott–Aldrich syndrome protein], formins, etc.) and its actin filament partner. The energy for force production

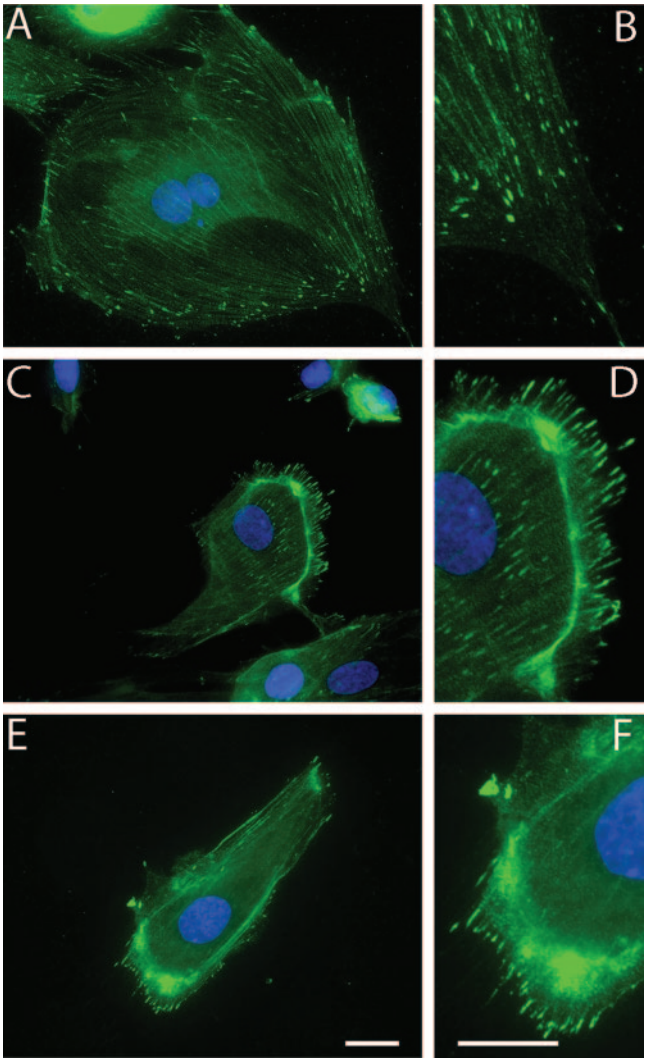

FIG. 4. CO- and NO-mediated VASP redistribution in HMECs. HMECs, cultured on fibronectin-coated coverslips, were treated with CO and NO donors as described in the legend to Fig. 1. *A* and *B*: Low- and high-power images of untreated cells showing uniform VASP localization on actin filaments throughout the cytoplasm. *C* and *D*: Low- and high-power images showing CO-induced VASP redistribution to filopodia at the leading edge of microvascular endothelial cells. *E* and *F*: Low- and high-power images showing NO-induced redistribution of VASP to filopodia. Representative results from three independent experiments are shown. Green, VASP; blue, DAPI (nuclei). Scale bars = 25 μm. (Please see http://dx.doi.org/10.2337/db08-0381 for a high-quality digital representation of this figure.)

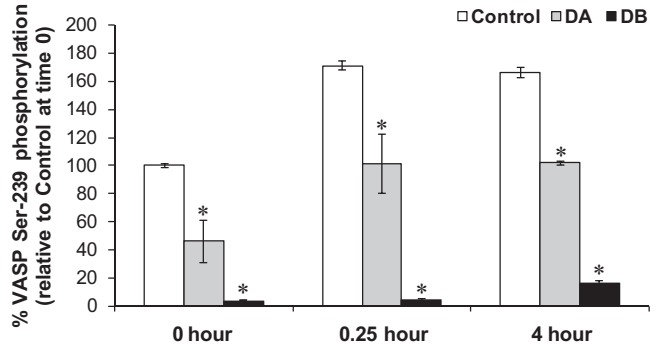

FIG. 5. NO exposure results in reduced VASP Ser-239 phosphorylation in diabetic $CD34^+$ cells compared with control cells. The extent of phosphorylation was determined by FACS analysis on $CD34^+$ cells from two diabetic subjects (DA [diabetic donor A] and DB [diabetic donor B]) and cells from a nondiabetic subject (Control [normal donor]). Values represent means ± SD. *$P < 0.05$.

appears to be derived from nucleotide hydrolysis at the filament's penultimate actin-ATP subunits, thereby promoting clampin release, translocation, and rebinding to terminal actin-ATP subunits. Before the active motor complex is assembled, clampins must be recruited to the membrane surface, where they dock at motility sites at the tips of filopodia and lamellipodia as well as in the focal adherens complex. Rottner et al. (23), for example, showed that VASP not only colocalizes to adhesion sites with the adaptor proteins vinculin and zyxin, but is also recruited to the tips of lamellipodia in amounts that are directly proportional to the rate of lamellipodial protrusion. Tokuo and Ikebe (26) further showed that myosin X specifically transports VASP and other members of the Ena/VASP clampin protein family to the leading edge, where VASP then binds to a membrane docking protein such as vinculin, zyxin, or migfilin (27,28). Only then can the actoclampin motor assemble and generate the forces needed for cell migration. When viewed from this perspective, VASP phosphorylation may affect the recruitment by myosin X, VASP docking with membrane components, and/or VASP-mediated formation of an active motor that can propel cell crawling. Moreover, as cells stop moving, VASP is known to redistribute to other intracellular sites. Benz et al. (29), for example, showed that VASP interacts with αII-spectrin in endothelial cells and that PKA-mediated VASP phosphorylation at Ser-157 inhibits this binding interaction. They also showed that VASP is dephosphorylated upon formation of cell-cell contacts and that, in confluent cells, αII-spectrin colocalizes with nonphosphorylated VASP at cell-cell junctions (29). The exact details of how VASP phosphorylation at Ser-157 or Ser-239 controls one or more of these steps remain to be worked out. Even so, the observation that different cell types contain various clampins and their respective membrane-docking proteins is likely to explain why VASP phosphorylation can either stimulate or suppress cell crawling and actin-based cell shape changes in a manner depending on cell type and/or culture conditions.

VASP is also the most abundant platelet and endothelial protein phosphorylated by PKG in NO signaling pathways, and, as noted above, this cytoskeletal adaptor protein is also a PKA substrate. Three serine/threonine phosphorylation sites within VASP play roles resulting in the inhibition of platelet aggregation and focal adhesion assembly (30,31). In this study, we demonstrated that CO can also regulate VASP phosphorylation, and we directly compare CO and NO effects in EPCs, platelets, and microvascular endothelial cells. We found that CO pretreatment can similarly stimulate EPC migration (Fig. 1) and phosphorylation of VASP's Ser-157, whereas NO exposure results in Ser-239 phosphorylation.

While we did not perform direct measurements of CO levels in our experiments, we did use CO concentrations that are achievable in vivo in physiological conditions and previously used by investigators (32,33). Endogenous CO has been reported to be generated in many cell types, and the amount of CO released via the heme oxygenase reaction can reach up to 12 ml/day ($\sim$16 $\mu mol \cdot l^{-1} \cdot h^{-1}$) (32). Previous studies have reported that tissues can produce 0.1–100 μmol/l CO in vivo from the HO reaction (33); it is therefore quite reasonable to believe that sufficient levels of HO-1 are present in cells to provide sufficient levels of CO, explaining our observed changes in VASP phosphorylation.

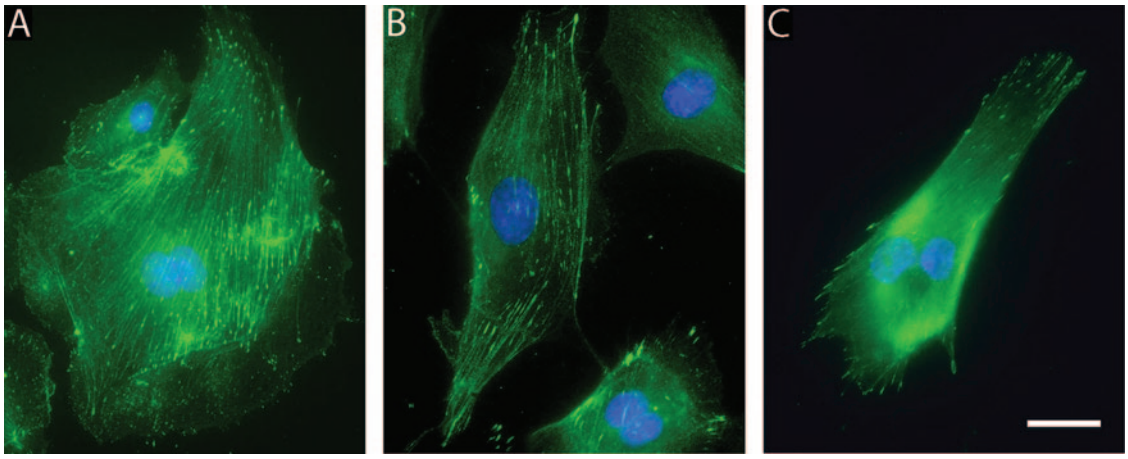

FIG. 6. Cell culture under high glucose (25 mmol/l) conditions attenuates CO- and NO-mediated VASP redistribution in HMECs. *A*: Untreated cells showing uniform VASP immunoreactivity along the actin filaments distributed throughout the cytoplasm. *B*: CO-induced VASP redistribution to leading-edge filopodia, albeit to an extent less than that observed at normoglycemic conditions (compare image with Fig. 3 graph). *C*: Less extensive VASP redistribution to filopodia in the presence of NO. Cells cultured for a week in 25 mmol/l glucose-supplemented medium on fibronectin-coated coverslips were either left untreated or treated with NO or CO (see legend to Fig. 1 for details) for 15 min before fixation and immunohistochemistry. Representative results from a minimum of three independent experiments are shown. Green, VASP; blue, DAPI (nuclei). Scale bar = 25 μm. (Please see http://dx.doi.org/10.2337/db08-0381 for a high-quality digital representation of this figure.)

Moreover, in response to incubation of microvascular endothelial cells with NO or CO donors, VASP was readily redistributed to the peripheral membrane and filipodia (Fig. 4). Thus, with regard to VASP localization, our data suggest that CO and NO may both have critical roles in vascular cell dynamics, and CO may have important contributions at low NO bioavailability, a condition already known to occur in diabetes. Our studies clearly indicate that both vasoactive gases promote cytoskeletal changes through site- and cell type-specific VASP phosphorylation and that responses to NO and CO are blunted in diabetes. While the migratory deficiency seen in diabetic EPCs could be overcome by exogenous NO (13), exogenous NO did not result in phosphorylation and redistribution of VASP in mature endothelial cells cultured in high glucose conditions. This defect can be viewed as "diabetes-induced NO resistance."

What also becomes apparent from the present study is that exposure of cells to NO or CO can greatly alter VASP recruitment to the leading edge with consequential effects on cell motility. Perhaps even more significant, in the context of diabetes, is that culturing endothelial cells at high glucose conditions that mimic diabetes results in motility defects that can be traced, at least in part, to altered VASP phosphorylation. We therefore postulate that these defects contribute to reduced vascular repair and tissue perfusion.

Both heme oxygenases generate CO, but they do so with very different kinetics (34,35); HO-1 is induced by oxidants such as hydrogen peroxide, UV radiation, and proinflam-

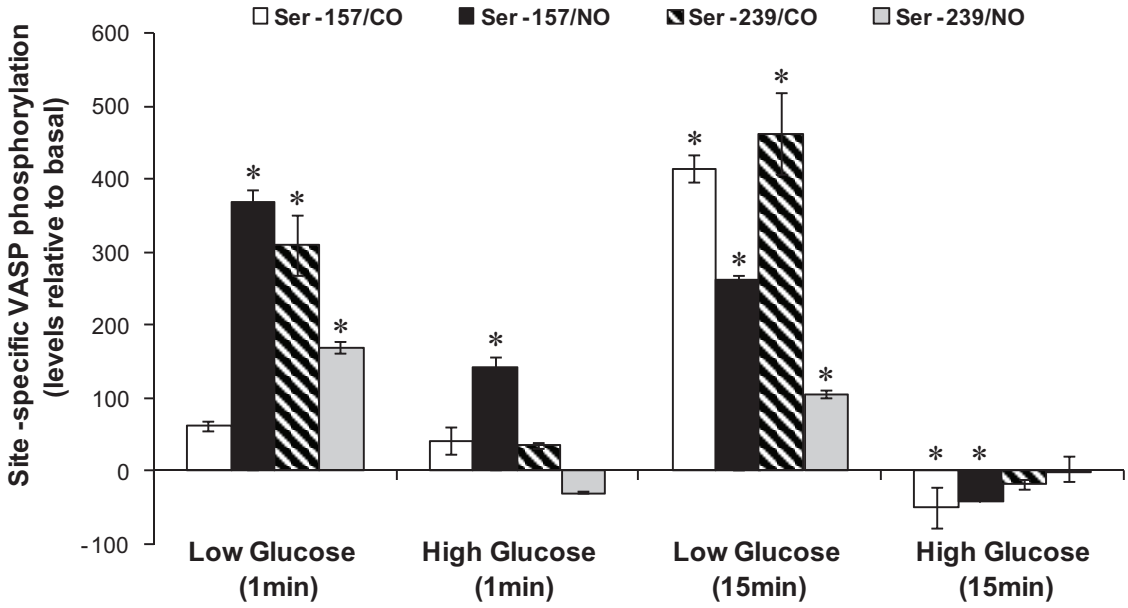

FIG. 7. Cell culture under high glucose (25 mmol/l) conditions blunts CO- and NO-mediated VASP phosphorylation in HMECs. HMECs were cultured in low (5.5 mmol/l) or high (25 mmol/l) glucose for 1 week, as described in RESEARCH DESIGN AND METHODS, before treatment with NO or CO donor at 37°C for 1 or 15 min (see legend to Fig. 1 for details). Cells were harvested in extraction buffer, and equal quantities of total protein were separated by SDS-PAGE, followed by transfer to nitrocellulose membrane and immunoblotting for VASP phosphorylation site determination and quantitative analysis (normalized to total VASP as a loading control). Basal levels represent no treatment in low glucose at 1 min. Representative results from three independent experiments are shown. Values represent means ± SD. *$P < 0.05$.

matory cytokines and by growth factors, hemodynamic or shear stress, heat shock, and even by NO (3). Endothelial cells derived from either the micro- or macrovasculature (36) responded equally to CO and NO, reflecting the key roles of both HO-1 and endothelial NO synthase throughout in the entire vasculature. In contrast, platelets do not respond to CO, perhaps reflective of the low levels of heme oxygenase in adult platelets (37). By altering HO-1 and NOS gene expression, hypoxia potentially modulates the availability of these gaseous second messengers. Thus, fluxes in the CO and NO generation during hypoxic stress are likely to have dramatic consequences on the regulation of vascular functions such as dilation, expression of vasomodulators, inhibition of platelet aggregation, and smooth muscle cell proliferation (38). Although the findings in this report support a role for CO sufficing for NO in promoting vascular cell migration, the signaling action of CO results in the phosphorylation of different VASP sites than NO. Furthermore, we demonstrate that, while both vasoactive gases promote cytoskeletal changes through site- and cell type–specific VASP phosphorylation, these responses are blunted in diabetes and may be responsible for the altered vascular repair and tissue perfusion associated with diabetic vascular complications.

ACKNOWLEDGMENTS

Support for this research came from National Institutes of Health Grants NIH1R01 EY07739 and NIHR01 EY12601 (to M.B.G.); the Juvenile Diabetes Research Foundation (to M.B.G.); and the American Heart Association (to S.L.C.).

We acknowledge Dr. Lynn Shaw for help in preparing the manuscript.

REFERENCES

1. Sikorski EM, Hock T, Hill-Kapturczak N, Agarwal A: The story so far: molecular regulation of the heme oxygenase-1 gene in renal injury. *Am J Physiol Renal Physiol* 286:F425–F441, 2004
2. Abraham NG, Kappas A: Pharmacological and clinical aspects of heme oxygenase. *Pharmacol Rev* 60:79–127, 2008
3. Ryter SW, Choi AM: Heme oxygenase-1: molecular mechanisms of gene expression in oxygen-related stress. *Antioxid Redox Signal* 4:625–632, 2002
4. Wink DA, Feelisch M, Fukuto J, Chistodoulou D, Jourd'heuil D, Grisham MB, Vodovotz Y, Cook JA, Krishna M, DeGraff WG, Kim S, Gamson J, Mitchell JB: The cytotoxicity of nitroxyl: possible implications for the pathophysiological role of NO. *Arch Biochem Biophys* 351:66–74, 1998
5. Maines MD: The heme oxygenase system: a regulator of second messenger gases. *Annu Rev Pharmacol Toxicol* 37:517–554, 1997
6. Furchgott RF, Jothianandan D: Endothelium-dependent and -independent vasodilation involving cyclic GMP: relaxation induced by nitric oxide, carbon monoxide and light. *Blood Vessels* 28:52–61, 1991
7. Duckers HJ, Boehm M, True AL, Yet SF, San H, Park JL, Clinton Webb R, Lee ME, Nabel GJ, Nabel EG: Heme oxygenase-1 protects against vascular constriction and proliferation. *Nat Med* 7:693–698, 2001
8. Morita T, Mitsialis SA, Koike H, Liu Y, Kourembanas S: Carbon monoxide controls the proliferation of hypoxic vascular smooth muscle cells. *J Biol Chem* 272:32804–32809, 1997
9. Nolan S, Dixon R, Norman K, Hellewell P, Ridger V: Nitric oxide regulates neutrophil migration through microparticle formation. *Am J Pathol* 172: 265–273, 2008
10. Xiao Q, Kiechl S, Patel S, Oberhollenzer F, Weger S, Mayr A, Metzler B, Reindl M, Hu Y, Willeit J, Xu Q: Endothelial progenitor cells, cardiovascular risk factors, cytokine levels and atherosclerosis: results from a large population-based study. *PLoS ONE* 2: e975, 2007
11. Zhang M, Zhou SH, Li XP, Shen XQ, Fang ZF: A novel hypothesis of atherosclerosis: EPCs-mediated repair-to-injury. *Med Hypotheses* 70:838–841, 2008
12. Liew A, Barry F, O'Brien T: Endothelial progenitor cells: diagnostic and therapeutic considerations. *Bioessays* 28:261–270, 2006
13. Segal MS, Shah R, Afzal A, Perrault CM, Chang K, Schuler A, Beem E, Shaw LC, Li Calzi S, Harrison JK, Tran-Son-Tay R, Grant MB: Nitric oxide cytoskeletal-induced alterations reverse the endothelial progenitor cell migratory defect associated with diabetes. *Diabetes* 55:102–109, 2006
14. Dickinson RB, Purich DL: Clamped-filament elongation model for actin-based motors. *Biophys J* 82:605–617, 2002
15. Gomez TM, Robles E: The great escape; phosphorylation of Ena/VASP by PKA promotes filopodial formation. *Neuron* 42:1–3, 2004
16. Reinhard M, Jarchau T, Walter U: Actin-based motility: stop and go with Ena/VASP proteins. *Trends Biochem Sci* 26:243–249, 2001
17. Deshane J, Chen S, Caballero S, Grochot-Przeczek A, Was H, Li Calzi S, Lach R, Hock TD, Chen B, Hill-Kapturczak N, Siegal GP, Dulak J, Jozkowicz A, Grant MB, Agarwal A: Stromal cell-derived factor 1 promotes angiogenesis via a heme oxygenase 1-dependent mechanism. *J Exp Med* 204:605–618, 2007
18. Ramamurthi A, Lewis RS: Measurement and modeling of nitric oxide release rates for nitric oxide donors. *Chem Res Toxicol* 10:408–413, 1997
19. Alberto R, Motterlini R: Chemistry and biological activities of CO-releasing molecules (CORMs) and transition metal complexes. *Dalton Trans* 17: 1651–1660, 2007
20. Dickinson RB, Caro L, Purich DL: Force generation by cytoskeletal filament end-tracking proteins. *Biophys J* 87:2838–2854, 2004
21. Halbrugge M, Friedrich C, Eigenthaler M, Schanzenbacher P, Walter U: Stoichiometric and reversible phosphorylation of a 46-kDa protein in human platelets in response to cGMP- and cAMP-elevating vasodilators. *J Biol Chem* 265:3088–3093, 1990
22. Jarchau T, Mund T, Reinhard M, Walter U: Purification and assays of vasodilator-stimulated phosphoprotein. *Methods Enzymol* 298:103–113, 1998
23. Rottner K, Behrendt B, Small JV, Wehland J: VASP dynamics during lamellipodia protrusion. *Nat Cell Biol* 1:321–322, 1999
24. Schatteman GC, Hanlon HD, Jiao C, Dodds SG, Christy BA: Blood-derived angioblasts accelerate blood-flow restoration in diabetic mice. *J Clin Invest* 106:571–578, 2000
25. Schatteman GC, Awad O: Hemangioblasts, angioblasts, and adult endothelial cell progenitors. *Anat Rec A Discov Mol Cell Evol Biol* 276:13–21, 2004
26. Tokuo H, Ikebe M: Myosin X transport Mena/VASP to the tip of filopodia. *Biochem Biophys Res Commun* 319:214–220, 2004
27. Purich DL, Southwick FS: ABM-1 and ABM-2 homology sequences: consensus docking sites for actin-based motility defined by oligoproline regions in Listeria ActA surface protein and human VASP. *Biochem Biophys Res Commun* 231:686–691, 1997
28. Zhang Y, Tu Y, Gkretsi V, Wu C: Migfilin interacts with vasodilator-stimulated phosphoprotein (VASP) and regulates VASP localization to cell-matrix adhesions and migration. *J Biol Chem* 281:12397–12407, 2006
29. Benz PM, Blume C, Moebius J, Oschatz C, Schuh K, Sickmann A, Walter U, Feller SM, Renne T: Cytoskeleton assembly at endothelial cell-cell contacts is regulated by alphaII-spectrin-VASP complexes. *J Cell Biol* 180:205–219, 2008
30. Walter U, Geiger J, Haffner C, Markert T, Nehls C, Silber RE, Schanzenbacher P: Platelet-vessel wall interactions, focal adhesions, and the mechanism of action of endothelial factors. *Agents Actions Suppl* 45:255–268, 1995
31. Smolenski A, Bachmann C, Reinhard K, Honig-Liedl P, Jarchau T, Hoschuetzky H, Walter U: Analysis and regulation of vasodilator-stimulated phosphoprotein serine 239 phosphorylation in vitro and in intact cells using a phosphospecific monoclonal antibody. *J Biol Chem* 273:20029–20035, 1998
32. Coburn RF, Williams WJ, Forster RE: Effect of erythrocyte destruction on carbon monoxide production in man. *J Clin Invest* 43:1098–1103, 1964
33. Nathanson JA, Scavone C, Scanlon C, McKee M: The cellular Na+ pump as a site of action for carbon monoxide and glutamate: a mechanism for long-term modulation of cellular activity. *Neuron* 14:781–794, 1995
34. Maines MD, Trakshel GM: Differential regulation of heme oxygenase isozymes by Sn- and Zn-protoporphyrins: possible relevance to suppression of hyperbilirubinemia. *Biochim Biophys Acta* 1131:166–174, 1992
35. Maines MD: Heme oxygenase: function, multiplicity, regulatory mechanisms, and clinical applications. *FASEB J* 2:2557–2568, 1988
36. Dulak J, Deshane J, Jozkowicz A, Agarwal A: Heme oxygenase-1 and carbon monoxide in vascular pathobiology: focus on angiogenesis. *Circulation* 117:231–241, 2008
37. Nowell SA, Leakey JE, Warren JF, Lang NP, Frame LT: Identification of enzymes responsible for the metabolism of heme in human platelets. *J Biol Chem* 273:33342–33346, 1998
38. Kourembanas S: Hypoxia and carbon monoxide in the vasculature. *Antioxid Redox Signal* 4:291–299, 2002